Specific single genes that carry nonsense mutations cause more than 2,400 distinctly inherited human diseases. Nonsense mutations are alterations in the genetic code that prematurely stop the translation process and lead to the production of incomplete non-functional proteins. These premature termination codons are depending on the disorder, account for 5-70% of the individual cases of genetic diseases including cystic fibrosis, hemophilia, methylmalonic acidemia, Rett syndrome and numerous types of cancer. DMD is also due to alteration of the *dystrophin* gene. These are premature termination codons account for up to 20% of patients. Despite advances in gene therapy, it is still far from achieving clinical success. An alternative, pharmacologic approach is to induce translational readthrough by suppressing the nonsense mutations using antibiotics. It has been reported that aminoglycoside antibiotics can decrease translational fidelity and cause readthrough of the in-frame premature termination signals. The fact that aminoglycosides could suppress nonsense mutations in cultured mammalian cells was first demonstrated by Burke and Mogg in 1985[3]. Gentamicin has been shown to suppress nonsense mutations and partially restore protein expression in *mdx* mouse, which carries a premature termination codon in the *dystrophin* gene[4]. However, aminoglycoside antibiotics are associated with numerous side effects such as auditory and renal malfunctions, and excessive use can lead to the emergence of drug-resistant bacteria.

Previously we reported that a dipeptide antibiotic negamycin that binds to the ribosomal decoding site and alters translational accuracy, successfully restored dystrophin expression with less toxicity than gentamicin in *mdx* mice[5,6]. Unfortunately, negamycin is unapproved drug for human use and it is difficult to synthesize in large quantities. In order to investigate more potent readthrough inducer with less toxicity and move readthrough efficiency with quantitative accuracy, we have established three transgenic mouse strain, named READ (Readthrough Evaluation and Assessment by Dual reporter), which expressed a dual-reporter gene[7]. In the present study, we tested several sterically related negamycin-like molecules searched by *in silico* screenings from over one million compounds and found two compounds, which have a beneficial effect on readthrough action. In addition, we demonstrated that these readthrough-inducing compounds promote the dystrophin re-expression by immunohistochemistry and reduction of serum CK activity in *mdx* mice.

2. Materials & methods

1) Chemicals

#3 ($C_{10}H_{14}N_2O_7$; (*E*)-4-(2,2-bis (2-methoxy-2-oxoethyl) hydrazinyl)-4-oxobut-2-enoic acid) and #4 ($C_8H_{15}N_3O_4$; 6-(2-hydrazinyl-2-oxoethanamido) hexanoic acid) were purchased from Hodogaya Contract Laboratory Co. Ltd. (Tsukuba, Japan). Gentamicin solution for injection was obtained from Schering-Plough K. K. (Tokyo, Japan) under the trade name Gentacin. Negamycin was a gift from Microbial Chemistry Research Foundation, Tokyo, Japan. All other chemicals were purchased from Sigma Aldrich Co. Ltd. (St. Louis, MO, USA) and Wako Pure Chemical Industries (Osaka, Japan).

2) *In silico* screening

Compounds structurally similar to negamycin were identified via chemical similarity searching. In similarity searching, each compound is assigned a "fingerprint" based on the types of atoms in the compound and the connectivity between those atoms (*e. g.* Atoms bonded to each other, atoms bonded to one of the atoms in the first bonded pair, and so on)[8-10]. The fingerprints of different compounds are then used to score the structural similarity between compounds based on the Tanimoto Similarity Index[11]. This procedure was performed on a database of over one million commercially available low-molecular weight compounds[12,13]. For the search, the Tanimoto Similarity Index was adjusted to approximately 50 compounds. Compounds were then purchased from the appropriate vendor. All calculations were performed using the Molecular Operating Environment (MOE, Chemical Computing Group).

3) Animals

READ mouse strain on a C57/BL6 background expressed a dual-reporter gene, which was composed of the *lacZ* and *luc* genes connected with a premature termination codon region derived from exon 23 of the *mdx* mouse *dystrophin* gene. Although the premature termination codon was originally TAA, we used TGA in the present study. For further details of this mouse, see Shiozuka *et al.*[7]. Male *mdx* and normal (C57/BL10) mice (5 weeks old; approximately 20 g body weight) were obtained from Japan SLC, Inc. The mice were housed individually under controlled conditions of temperature and humidity and had free access to water and food. All experiments using mice were conducted under the approval of

the University of Tokyo Animal Ethics Committee.

4) Readthrough analysis on READ mice

READ mice (8 weeks old ; approximately 20 g body weight) were injected subcutaneously with 0.2 ml of compound in saline daily for 7 days. At the completion of the administration, the mice were euthanized with an overdose of ether. Tissue samples were collected from the rectus femoris, gastrocnemius and soleus. Dissected tissues were minced with scissors and homogenized in three volumes of the reporter lysis buffer (Promega, Madison, WI, USA) using a tissue grinder (Physcotron ; Niti-on, Japan). Tissue homogenates were subjected to one round of freeze-thawing. The lysate supernatants were collected after centrifugation at 17,710×*g* for 10 min, and then analyzed using the Beta-Glo and Bright-Glo luciferase assay systems (Promega). The ß-galactosidase and luciferase activities were measured according to the manufacturers' instructions using a luminometer (Luminescencer-JNRII AB-2300 ; Atto, Japan). The readthrough efficiency was determined as the ratio of luciferase activity to ß-galactosidase activity.

5) Immunohistochemical and Biochemical analysis on *mdx* mice

Mdx mice were injected subcutaneously with compound (1 mg/day) in saline (0.2 ml) daily for 21 days. Staining of dystrophin in muscle tissues was carried out on 8 μm transverse cryosections as described Welch *et al.*[14]. The sections were stained with a rabbit polyclonal antibody against C-terminus of dystrophin (ab-15277 ; Abcam Inc., Cambridge, MA, USA) diluted 1 : 1000 in 10% bovine serum albumin and detected with Alexa Fluor 488 secondary antibody (Molecular Probes Inc., Eugene, OR, USA) diluted 1 : 750 in 10% bovine serum albumin. Specimens were examined under a fluorescence microscope (Axioplan, Carl Zeiss GmbH, Oberkochen, Germany). The images were optimized for contrast and brightness using Photoshop CS3 software (Adobe Inc., San Jose, CA, USA).

Blood samples were collected by direct heart puncture under anesthesia and allowed to flow into tubes without anticoagulant for 30 min. Samples were then centrifuged at 2,500×*g*, 4℃, for 10 min ; and the supernatants were assayed using an automated blood sample analyzer (Fujifilm DRI-CHEM 3500s ; Fujifilm Medical Co. Ltd, Japan).

3. Results & discussion

We screened computationally to searching novel readthrough-inducing molecules from a

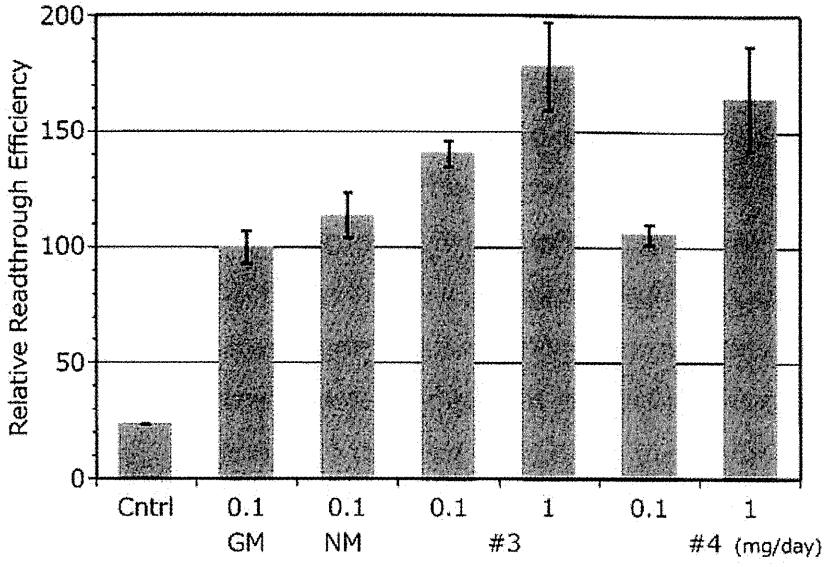

Fig. 2 Effects of readthrough-inducing molecules on READ mice

The readthrough activities following single, daily subcutaneous injections were compared with GM (gentamicin) and NM (negamycin). Cntrl (control) means the mice administrated with saline. Error bars indicate SDs.

data bank with 1,053,207 compounds, and picked up 29 compounds. Among them, we examined 19 compounds by injecting into READ mice to assess readthrough activity and found some newly identified compounds, which could induce readthrough. The dual reporter construct of READ mouse was composed of the *lacZ* and *luc* genes connected with a premature termination codon region. Although the premature termination codon of the *mdx* mouse was originally TAA, we adopted TGA-centered sequences because previous study indicated that aminoglycoside antibiotics tend to exhibit the highest readthrough activity for TGA[15]. When a test substance with no readthrough activity was administered to READ mice, only ß-galactosidase was translated. The readthrough efficiency was determined as the ratio of luciferase activity to ß-galactosidase activity.

1) Effects of readthrough-inducing molecules on READ mice

The readthrough activities of compound #3 and #4 were compared with gentamicin and negamycin that were treated by daily subcutaneous administration for 7 days (**Fig. 2**). Both compound #3 and #4 exhibited readthrough activity which is equal to gentamicin or negamycin known as readthrough-inducing molecules. As for compound #4, there was no decrease in body weight, no pathological changes by autopsy, and no abnormal value on

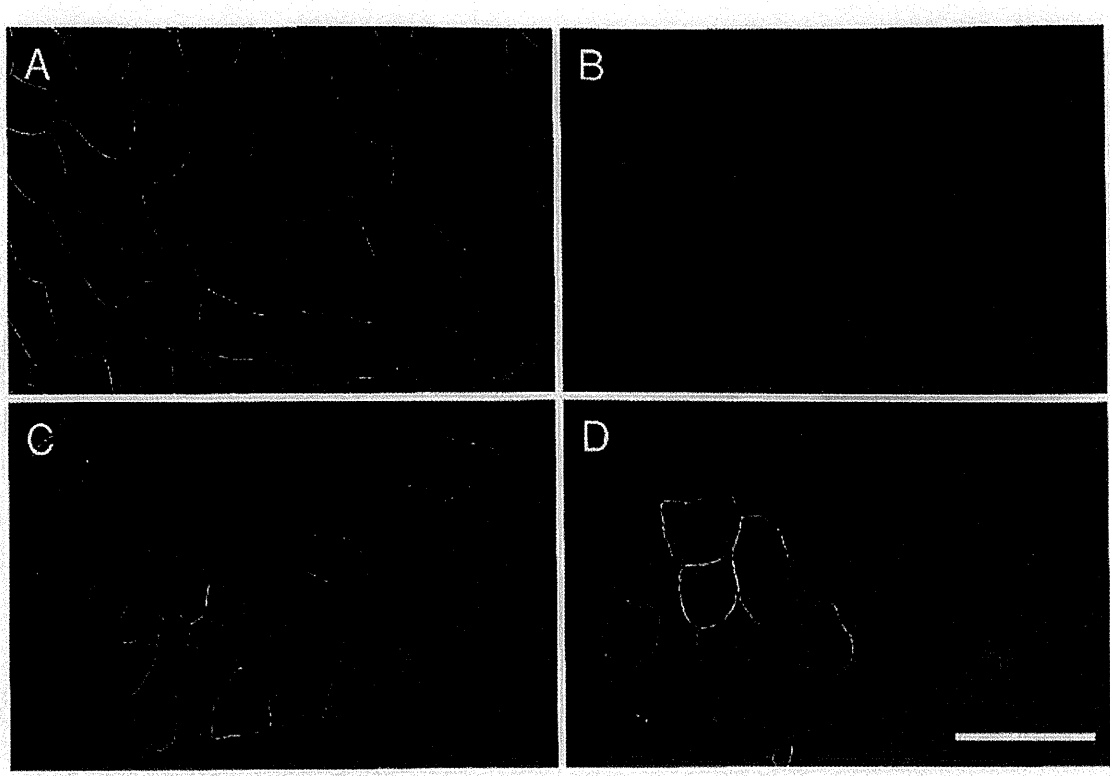

Fig. 3 Effects of #3 and #4 treatment on dystrophin expression

Immunohistochemistry of B10 (A) and *mdx* (B-D) skeletal muscle. The presence of dystrophin was detected by pAb to the COOH-terminus of dystrophin. Dystrophin was present in B10 muscle (A) and in *mdx* muscle treated with #3 (C) or #4 (D) in 3 weeks treated with 1 mg/body/day. No dystrophin was detected in untreated *mdx* muscle (B). Bar = 100 um

serum biochemistry test (22 items ; Albumin, Alanine aminotransferase, Alkaline phosphatase, Amylase, Aspartate aminotransferase, Blood urea nitrogen, Creatine kinase, Creatinin, Gamma-glutamyl transpeptidase, Glucose, High density lipoprotein-cholesterol, Lactose dehydrogenase, Na^+, K^+, Cl^-, Ca^{2+}, P^+, Phospholipid, Total Bilirubin, Total cholesterol, Total protein, Triglyceride) in ICR mice reared in a specific pathogen-free animal facility treated with intraperitoneal injection daily for 14 days up to 250 mg/kg/day (data not shown). Moreover, we confirmed that compound #4 promoted readthrough activity by oral administration as well in READ mice (data not shown).

2) Effects of #3 and #4 treatment on dystrophin expression

To determine whether both compounds could lead to suppression of the premature termination codon in dystrophin of *mdx* mice, compound #3 or #4 were treated by daily subcutaneous injection (50 mg/kg/day) for 21 days. Immunohistochemistry of muscle cross-sections to view dystrophin showed in **Fig. 3**. Administered compounds resulted in

synthesis of full-length dystrophin and its proper localization only in treated *mdx* mice. The dystrophin positive fibers in *mdx* mice treated with compound #3 or #4 had approximately 16.2% (84/523) or 18.8% (65/345) respectively. Hoffman *et al.* reported that in several cases of mild Becker muscular dystrophy, the phenotype was improved by dystrophin expressed at a level greater than or equal to 20% of normal[16]. Although we have no direct evidence as to whether normal dystrophin level observed in this study would be sufficient to improve muscle performance *in vivo*, it is likely to be far better than a complete lack of dystrophin.

Previous studies have shown that aminoglycosides suppress various stop codons with dramatically different efficiencies (UGA>UAG>UAA) and that the effectiveness of suppression is further dependent upon the identity of the first nucleotide immediately downstream from the stop codon (C>U>A/G) and the local sequence context around the stop codon[15]. The premature termination codon "UAA A" is found in the *dystrophin* gene of the *mdx* mouse and is lowest readthrough efficiency.

3) Effects of #3 and #4 treatment on CK activity

In blood samples, a high level of activity of the enzyme CK is another index of sarcolemmal fragility widely used as a diagnostic biochemical marker for muscular dystrophy[1]. To obtain a further indication of the degree of protection resulting from treatment of both compounds, we examined serum CK accumulation on *mdx* mice treated for 21 days. As shown in **Fig. 4**, Compounds #3 and #4 exhibit significantly reduced CK activities and its value was almost half. Thus, the level of protection afforded by the chemotherapy was functionally significant.

In conclusion, our results demonstrate that both compounds induce readthrough of the premature termination codon, resulting in the partial restoration of dystrophin protein and in the reduction of creatine kinase activity in *mdx* mice. These results demonstrate the feasibility of these investigational drugs to DMD and suggest that both compounds represents an important chemical entity for the potential treatment of genetic disorders caused by nonsense mutations. These novel chemotherapeutic agents that overrides premature termination codons may provide significant therapeutic value in treating or preventing genetic diseases associated with nonsense mutations. Readthrough-induced molecules have therapeutic potential for nearly one-third of all genetic disorders. These molecules may achieve even better rescue from DMD with lower toxicity and form the basis of the effective therapy for other inherited diseases involving nonsense mutations.

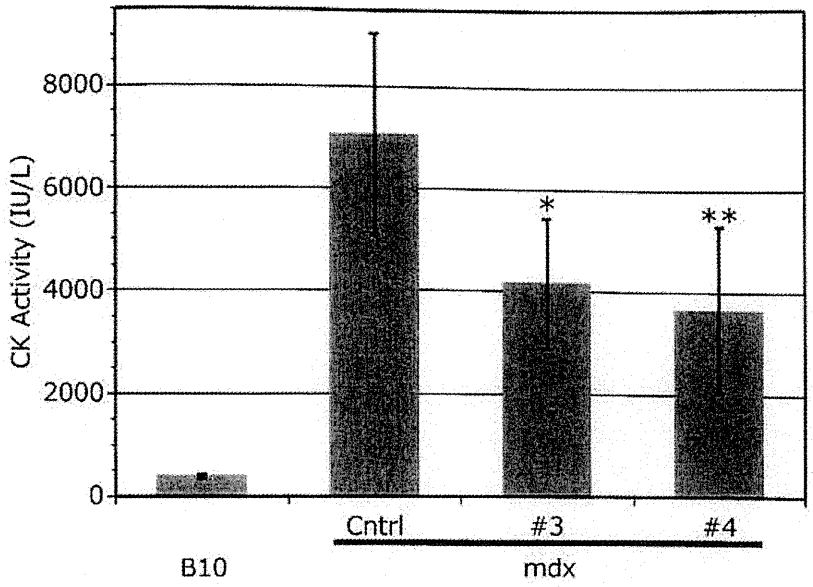

Fig. 4 Effects of #3 and #4 treatment on CK activity

Serum CK activities were dropped significantly in *mdx* mice treated for 3 weeks. $^{*}p=0.056$ (vs. Cntrl), $^{**}p=0.039$ (vs. Cntrl).

Acknowledgments

This work was supported in part by The Ichiro Kanehara Foundation (to MS), Health and Labour Sciences Research Grant for Research on Psychiatric and Neurological Diseases and Mental Health (19A-020 ; to RM), Comprehensive Research on Disability Health and Welfare (H22-ShinkeiKin-Ippan-016 ; to RM), Nervous and Mental Disorders (20B-13 ; to RM) from the Ministry of Health, Labour and Welfare, Japan.

References

1) Ebashi S, Toyokura Y, Mimoi H, Sugita H. High creatine phosphokinase activity of sera of progressive muscular dystrophy. J Biochem. 1959 ; 46 : 103-104.
2) Matsuda R, Nishikawa A, Tanaka H. Visualization of dystrophic muscle fibers in mdx mouse by vital staining with Evans blue : evidence of apoptosis in dystrophin-deficient muscle. J Biochem. 1995 ; 118 : 959-964.
3) Burke JF, Mogg AE. Suppression of a nonsense mutation in mammalian cells in vivo by the aminoglycoside antibiotics G-418 and paromomycin. Nucleic Acids Res. 1985 ; 13 : 6265-6272.
4) Barton-Davis ER, Cordier L, Shoturma DI, Leland SE, Sweeney HL. Aminoglycoside antibiotics restore dystrophin function to skeletal muscles of mdx mice. J Clin Invest. 1999 ; 104 : 375-381.
5) Arakawa M, Nakayama Y, Hara T, Shiozuka M, et al. Negamycin can restore dystrophin in *mdx* skeletal muscle. Acta Myol. 2001 ; 20 : 154-158.
6) Arakawa M, Shiozuka M, Nakayama Y, Hara T, Hamada M, Kondo S, Ikeda D, Takahashi Y, Sawa R, Nonomura Y, Sheykholeslami K, Kondo K, Kaga K, Kitamura T, Suzuki-Miyagoe Y, Takeda S,

Matsuda R. egamycin restores dystrophin expression in skeletal and cardiac muscles of mdx mice. J Biochem. 2003 ; 134 : 751-758.
7) Shiozuka M, Wagatsuma A, Kawamoto T, Sasaki H, Shimada K, Takahashi Y, Nonomura Y, Matsuda R. Transdermal delivery of a readthrough-inducing drug : a new approach of gentamicin administration for the treatment of nonsense mutation-mediated disorders. J Biochem. 2010 ; 147 : 463-470.
8) Brown RD, Martin YC. The infomation content of 2D and 3D structural descriptions relevant to ligand-receptor binding. J Chem Inf Comp Sci. 1997 ; 37 : 1-9.
9) Godden JW, Xue L, Bajorath J. Combinatorial preferences affect molecular similarity/diversity calculations using binary fingerprints and Tanimoto coefficients. J Chem Inf Comput Sci. 2000 ; 40 : 163-166.
10) Godden JW, Stahura FL, Bajorath J. Anatomy of fingerprint search calculations on structurally diverse sets of active compounds. J Chem Inf Model. 2005 ; 45 : 1812-1819.
11) Butina D. Unsupervised data base clustering on daylight's fingerprint and Tanimoto similarity : A fast and automated way to cluster small and large data sets. J Chem Inf Comp Sci. 1999 ; 39 : 747-750.
12) Pan Y, Huang N, Cho S, MacKerell AD Jr. Consideration of molecular weight during compound selection in virtual target-based database screening. J Chem Inf Comput Sci. 2003 ; 43 : 267-272.
13) Macias AT, Mia MY, Xia G, Hayashi J, MacKerell AD Jr. Lead validation and SAR development via chemical similarity searching : application to compounds targeting the pY+3 site of the SH2 domain of p56lck. J Chem Inf Model. 2005 ; 45 : 1759-1766.
14) Welch EM, Barton ER, Zhuo J, Tomizawa Y, Friesen WJ, Trifillis P, Paushkin S, Patel M, Trotta CR, Hwang S, Wilde RG, Karp G, Takasugi J, Chen G, Jones S, Ren H, Moon YC, Corson D, Turpoff AA, Campbell JA, Conn MM, Khan A, Almstead NG, Hedrick J, Mollin A, Risher N, Weetall M, Yeh S, Branstrom AA, Colacino JM, Babiak J, Ju WD, Hirawat S, Northcutt VJ, Miller LL, Spatrick P, He F, Kawana M, Feng H, Jacobson A, Peltz SW, Sweeney HL. PTC124 targets genetic disorders caused by nonsense mutations. Nature. 2007 ; 447 : 87-91.
15) Howard MT, Shirts BH, Petros LM, Flanigan KM, Gesteland RF, Atkins JF. Sequence specificity of aminoglycoside-induced stop condon readthrough : potential implications for treatment of Duchenne muscular dystrophy. Ann Neurol. 2000 ; 48 : 164-149.
16) Hoffman EP, Kunkel LM, Angelini C, Clarke A, Johnson M, Harris JB. Improved diagnosis of Becker muscular dystrophy by dystrophin testing. Neurology. 1989 ; 39 : 1011-1017.

1 9

2 Effects of Dietary Phosphate on Ectopic 3 Calcification and Muscle Function in mdx Mice

4 Eiji Wada, Namiko Kikkawa, Mizuko Yoshida,
5 Munehiro Date, Tetsuo Higashi and Ryoichi Matsuda
6 *The University of Tokyo,*
7 *Japan*

8 1. Introduction

9 Calcium deposits in extra-skeletal tissues are highly correlated with lifestyle diseases. The
10 mechanisms and clinical effects of such deposition have been widely studied due to increase
11 mortality rate. Vascular calcification is a major complication in a number of diseases, including
12 chronic kidney disease (CKD) and diabetes (Giachelli, 2009). The number of regulation
13 mechanisms affecting calcium precipitation in soft tissues remains underestimated, as many
14 regulators are considered to be involved in this complex process (Hu et al., 2010; Kendrick et
15 al., 2011). Elevated serum phosphate levels which leads hyperphosphatemia is one of the
16 prevalent factors of vascular calcification in CKD (El-Abbadi et al., 2009). The kidneys play a
17 central role in the regulation of phosphate homeostasis. In individuals with normal renal
18 function, serum phosphate levels are strictly controlled through dietary intake, intestinal
19 absorption, renal excretion, and bone metabolism. When the kidneys are either mechanically
20 or functionally impaired, phosphate metabolism is imbalanced. Abnormalities of phosphate
21 metabolism related to kidney malfunction may play a central role in the deposition of calcium
22 and phosphate in extra-skeletal tissues. Ectopic calcification in skeletal muscle has been
23 reported to occur in three Duchenne muscular dystrophy (DMD) animal models; mdx mice
24 (Coulton et al., 1987; Kikkawa et al., 2009), dystrophic puppies (Nguyen et al., 2002), and
25 hypertrophic muscular dystrophy cats (Gaschen et al., 1992). In this chapter, we review the
26 mechanisms of ectopic calcification in mdx mice and report a new finding of effects of dietary
27 phosphate intake on calcium deposits and muscle function in mdx mice.

28 2. Ectopic calcification in animal models of muscular dystrophy

29 The mdx mouse, dystrophic canine, and hypertrophic muscular dystrophy feline develop
30 progressive muscle lesions and calcium deposits in skeletal muscle during muscle
31 regeneration. The pathological features of dystrophic golden retriever puppies are particularly
32 severe and are similar to those of DMD boys, who are characterized by progressive muscle
33 necrosis that leads to early death. Nguyen et al. (2002) detected early ectopic calcification in
34 muscles from 4-day-old and 2-month-old puppies. Thus calcium deposition in skeletal muscle
35 appears to be an early event associated with muscle degeneration.

36 In mdx mice, the observed muscle pathology is relatively mild compared with DMD patients
37 but calcifying lesions are commonly seen in the lower limbs and diaphragm of mice from

approximately five weeks of age. Recently, ectopic calcification (Fig. 1) has been reported to be a characteristic feature of muscular pathology (Korff et al., 2006; Verma et al., 2010). For example, Korff et al. (2006) found that myocardial calcification commonly occurs in mice following necrosis induced by mechanical stresses and proposed that calcification in the heart is dependent upon genetic background. Verma et al. (2010) suggested that the absence of ectopic calcification in the diaphragm serves as a marker of amelioration of mdx pathology. In addition, one of the prednisone-induced side effects in a canine model of DMD is skeletal muscle calcification (Liu et al., 2004). However, a palliative glucocorticoid therapy using prednisone is a feasible and effective treatment approach for DMD despite of the serious potential side effects (Wong et al., 2002; Khan, 1993). Studies in these animals have revealed that the percentages of calcified myofibers in necrotic lesions increases dose dependently. It is speculated that calcium deposits in skeletal muscle are occurred as results of abnormal calcium and phosphate homeostasis and delayed muscle degeneration and regeneration cycle.

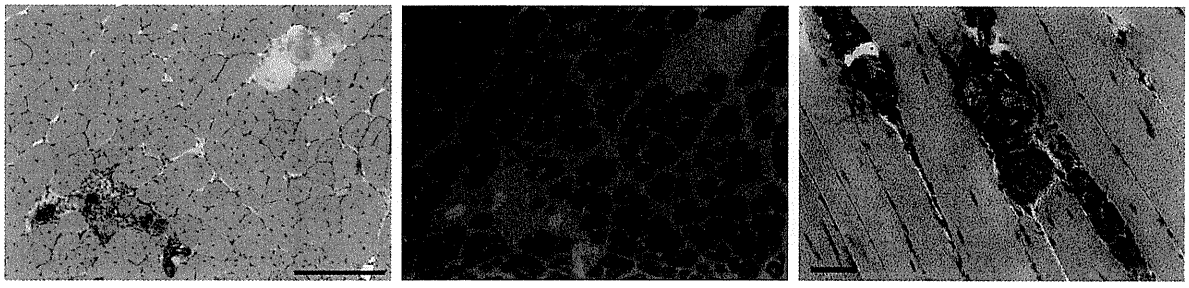

Fig. 1. Ectopic calcification in mdx mice (90 days old). Transverse (left and center) and longitudinal (right) sections, stained with H&E (left and right) and Evans blue (center). The bar represents 10 μm.

3. Identification of calcium deposits in mdx mice skeletal muscle

Our group is actively studying ectopic calcification in mdx mice skeletal muscle (Kikkawa et al., 2009). We performed experiments with 90-day-old mdx and control mice (C57BL/10: B10) fed a commercial standard chow (CE-2; Clea Japan, Tokyo, Japan) and water *ad libitum*. Following sacrificed of the mice, high-resolution X-ray micro-computed tomography (CT) imaging of the hind limbs of mdx and B10 mice using a SkyScan-1074 scanner (SkyScan, Kontich, Belgium) revealed that all mdx mice had muscle calcification in the hind limb, whereas no calcium precipitation was observed in the control mice (Fig. 2).

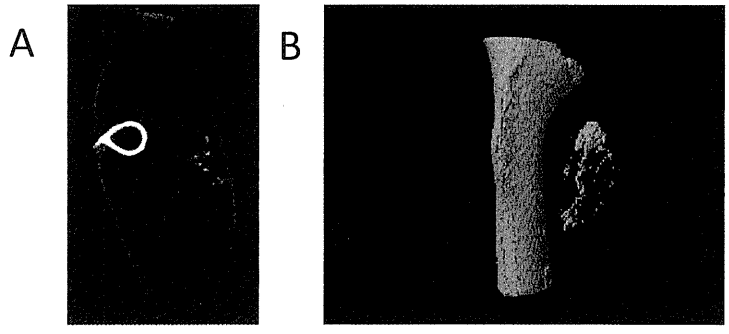

Fig. 2. Images of the hind limb of a two-month-old mdx mouse. X-ray-absorbing materials are shown as gray shadows and the femeur can be seen in the center of the X-ray image. (A) CT image. (B) Reconstructed 3D image. (Kikkawa et al., 2009)

The main composition of calcium deposits in the skeletal muscle was identified using an back-scattered electron imaging and energy-dispersive X-ray spectrometry (EDS) analysis by S-4500 SEM (Hitachi, Tokyo, Japan). In a cross-section of the muscle from an mdx mouse, spotty and bright crystals were observed. The EDS spectra obtained from the crystals indicated the presence of both calcium and phosphorus (Fig. 2A-B). To determine whether the composition of the deposits consisted of a calcium phosphate phase, muscle samples were analyzed using a JEM-2010 TEM (JEOL, Tokyo, Japan) equipped with an EDS detector. The electron diffraction pattern from an obtained TEM image of the specimen nearly was an identical match with a simulated diffraction pattern of hydroxyapatite (Ca5(PO4)3OH; HA) (Fig. 3C). Based on these results, we concluded that the calcification of mdx skeletal muscles is due to the precipitation of hydroxyapatite.

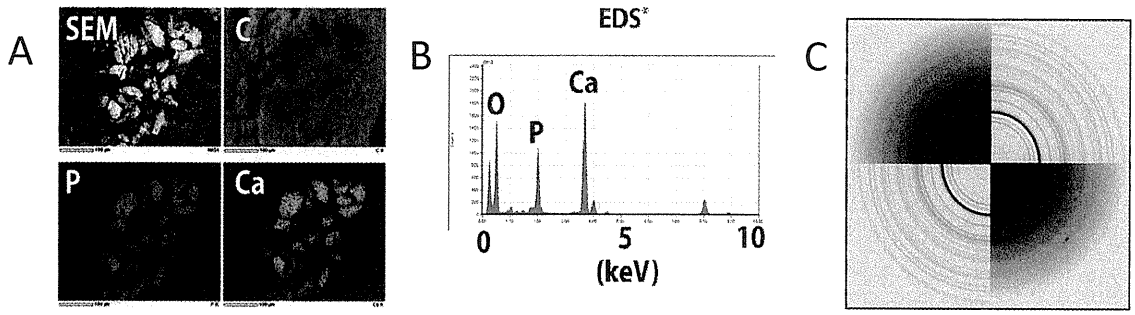

Fig. 3. SEM and TEM analyses of ectopic calcification in mdx mice skeletal muscle. (A) Electron probe microanalysis identified the particles as calcium phosphate. (B) Energy dispersive X-ray spectroscopy. (C) Identical match of X-ray diffraction of the particles and HA. (Kikkawa et al., 2009).

4. Serum biochemistry of mdx and B10 mice fed a commercial diet

As we determined that ectopic calcification is composed of HA, the main component of bones, we suspected that mdx mice have a metabolic disorder of calcium (Ca) and phosphate (Pi) homeostasis. To examine the levels of Ca and Pi in blood, serum samples were collected from two-month-old mdx and B10 mice fed a commercial diet (CE-2 containing 1.0 g/100 g Pi and 1.0 g/100 g Ca) and water *ad libitum*. The two minerals were measured using an automated clinical chemistry analyzer Fuji Dri-chem 4000 (Fujifilm, Tokyo, Japan). Comparison of the serum mineral components of mdx and B10 mice revealed that mdx mice had significantly higher serum Pi levels (1.41 fold; $P<0.05$) than the control mice, whereas no significant differences in serum Ca levels were detected. These results are supported by a previous study in mdx and B10 mice by Brazeau et al. (1992).

The concentrations of serum fibroblast growth factor-23 (FGF-23), which is an important regulator of phosphorus, were also measured using an FGF-23 ELISA kit (Kainos Laboratories, Tokyo, Japan). The serum level of FGF-23 of mdx mice was significantly higher (1.5 fold; $P<0.05$) than that of B10 mice.

Nearly all of the identified functions of FGF-23 are activated or operate through Klotho, a single transmembrane protein of the β-glycosidase family that is expressed in the distal kidney tubules and parathyroid gland (Kuro-o, 2010). Both FGF-23 and Klotho have emerged as responsible factors for mediating phosphate homeostasis. It has been reported

that soft tissue calcification and hyperphosphatemia are observed in mice lacking either FGF-23 (Razzaque et al., 2006) or Klotho (Kuro-o et al., 1997). Klotho mutant mice also exhibit multiple age-associated disorders, such as arteriosclerosis, osteoporosis, short-life span, and ectopic calcification. However, as these phenotypes are rescued by the restriction of dietary phosphorus alone in male Klotho mice (Morishita et al., 2010) we predicted that the amount of dietary Pi intake influences the precipitation of calcium in mdx mice, and that the restriction of dietary Pi may improve mdx muscle pathology and function.

5. Influence of phosphate diet

Based on our findings that mdx mice have calcium deposits composed of HA and exhibit higher serum phosphate levels, we speculated that dietary phosphate intake might modulate ectopic calcification in mdx mice. To test this speculation, mdx mice and B10 mice were divided into three diet groups (n=30) from weaning (20 days old) that were fed diets with Pi contents of 2.0 g/100 g (high-Pi diet), 1.0 g/100 g (mid-Pi diet), and 0.7 g/100 g (low-Pi diet) manufactured by Oriental Yeast Company (Tokyo, Japan). Other ingredients, including calcium (1.2 g/100 g) in the diets were present in the same amounts among the groups. The experimental diets were based on the CE-2 and mid-Pi diet was a same composition with CE-2 diet which was fed to pregnant and nursing mice of both genotypes. All mice were housed in cages with pulp bedding (Palmas-μ; Material Research Center, Tokyo, Japan) in a controlled room with a 12-h light/dark cycle and a temperature of 25℃. The experimental chows and water were available *ad libitum*. Mice were either sacrificed with an overdose of diethylether at age 30, 60, or 90 days or used for measurements of muscular function at age 60 days. Twenty-four hours before euthanasia, mice were received an intraperitoneal injection of Evans blue dye (EBD, 100 mg/kg) which incorporates into regenerating myofibers with permeable membranes (Matsuda et al., 1995). All procedures were performed in accordance with the ethical guidelines of the University of Tokyo.

5.1 Changes in ectopic calcification in skeletal muscle

Changes in ectopic calcification in mdx mice skeletal muscle induced by dietary phosphate content were observed using a modified whole body double-staining method involving alizarin red S and alcian blue, which stain bones and cartilage respectively (Dingerkus et al., 1977; McLeod, 1980; Webb et al., 1994). Briefly, 90-day-old mice were sacrificed and fixed in 95% ethanol (EtOH) for 7 days after the skin and organs were removed. The EtOH was then replaced in acetone and the samples were further incubated for 3~4 days. After partial drying, samples were stained in a mixed solution of 0.3% alcian blue 8GX (Fluka, Germany) in 70% EtOH, 0.1% alizarin red S (WAKO, Osaka, Japan) in 95% EtOH, and 2.0% potassium hydrogen phthalate in 70% EtOH for 3 days. Each stained mouse was washed in distilled water and placed in 0.75% potassium hydroxide (KOH) in MilliQ water for 2 days to initiated maceration and clearing. Clearing was continued by adding increasing concentration of glycerol (20%, 50%, 70% and 100%) in 0.75% KOH to obtain a completely cleared specimen (Fig. 4A). Calcified regions were stained reddish violet, similar to appearance of stained bones.

Imaging of the stained and cleared samples showed that no bone-like red staining was present in the skeletal muscles of B10 mice fed any of the three phosphate diets (Fig. 4A-a). However, in mid-Pi fed mdx mice, striped and spotty red stained areas, particularly in the

back, gluteus, and lower limbs muscles, were detected (Fig. 4A-b), while excessive calcification was clearly observed in the samples from high-Pi fed mdx mice (Fig. 4A-c, Fig. 4B). The staining revealed severe calcification, particularly in the diaphragm, back, gluteus, and lower limbs muscles, where severely degenerated muscle fibers were visible macroscopically by EBD staining (Fig. 4C). In contrast, bone-like red staining was rarely seen in the whole bodies of the low-Pi fed mdx mice (Fig. 4A-d, Fig. 4B).

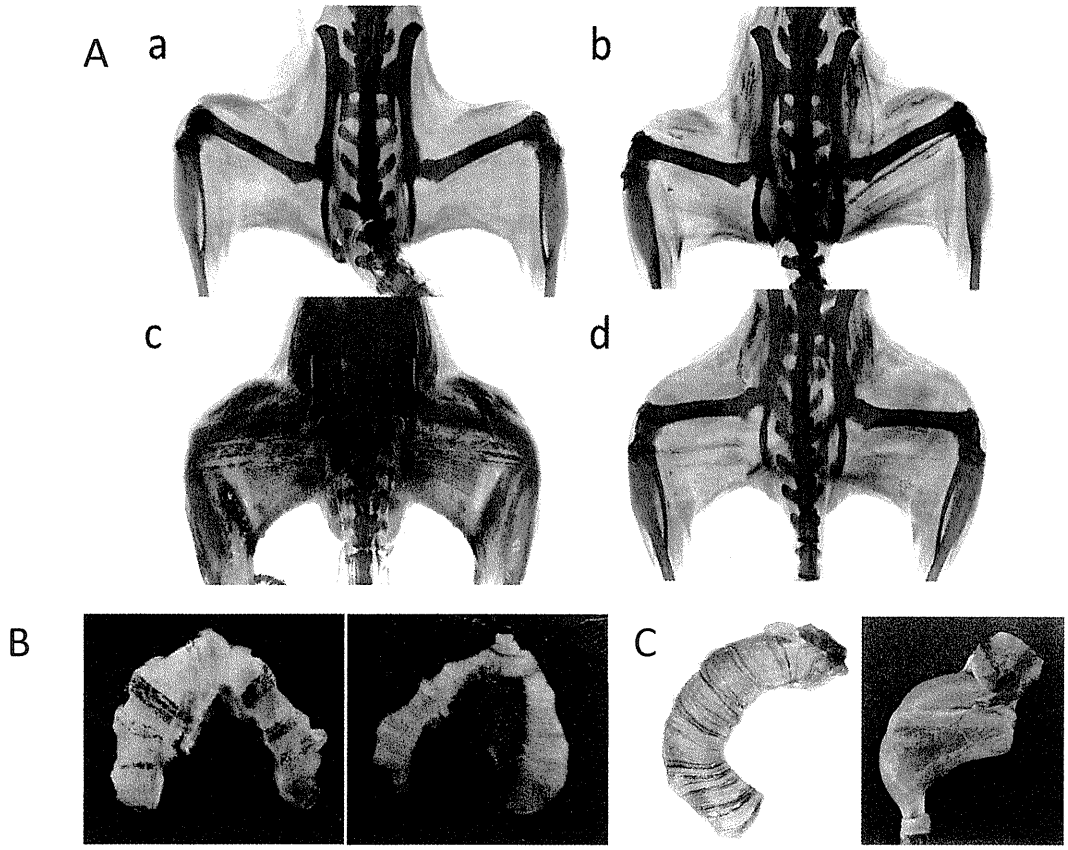

Fig. 4. Results of whole-body double staining of mdx and B10 mice, and Evans blue dye staining of mdx mice. (A) Images of the whole-body double staining of the lower body. (A-a) Lower body of a B10 mouse fed a high-Pi diet. The lower body of mdx mice (A-b) fed a mid-Pi diet, (A-c) high-Pi diet and (A-d) low-Pi diet. (B) Pictures of the whole body double staining of diaphragm. Diaphragm of an mdx mouse fed a high-Pi diet (left) and low-Pi diet (right). (C) Evans blue dye in the diaphragm (left) and lower limb (right) of an mdx mouse. Evans blue-positive lesions are seen in blue.

Quadriceps muscle samples from low-Pi, mid-Pi, and high-Pi fed mdx mice at 30, 60, and 90 days of age were sectioned at 8 μm thickness to determine the onset of calcifying lesions. Hematoxylin and eosin (H&E) and alizarin red S (1%) staining were used to observe pathology and detect calcification in the samples (Fig. 5). Histology showed early mineralization in degenerating myofibers in high-Pi fed mdx mice at 30 days of age (only fed a high-Pi diet only for 10 days), whereas no alizarin red-positive areas were present in either mid-Pi or low-Pi fed mdx mice of the same age. In addition, few calcium deposits were seen in mid-Pi fed mdx mice by the age of 60 days or in low-Pi fed mdx mice even by

90 days of age. Calcium deposits were extensive throughout the entire sections of high-Pi fed mdx mice at 90 days of age.

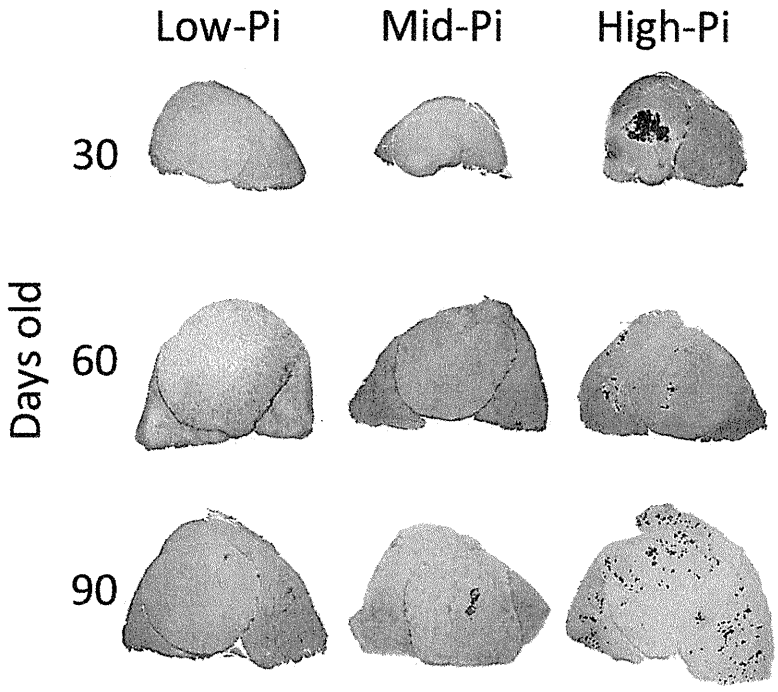

Fig. 5. Alizarin red S-stained cryosections of mdx mice quadriceps muscle. Calcium deposits are stained red.

5.2 Ectopic calcification in other tissues

Although the presence of calcification is rarely reported in organs of mdx mice other than skeletal muscle, including the heart and kidneys, these mice exhibit abnormal cardiac pathology and function (Zhang et al., 2008) and their myocardium is vulnerable (Costas et al., 2010). Rodent models of muscular dystrophies may have potential for sensitivity to myocardial calcification when challenged by mechanical or chemical stressors, because such calcification is commonly observed in the hamster model of muscular dystrophy (Burbach, 1987). For instance, Elsherif et al. (2008) found that dystrophin and β1 integrin double-knockout mice (β1KOmdx) show exacerbated myocardiopathy and extensive calcification in the heart, particularly under pregnancy-induced stress. Thus we predicted that high-Pi intake would also affect calcification in the myocardium of mdx mice.

Calcification in the heart was evaluated by 8 μm cryosections of samples from the three Pi-diet group mice. We found that high-Pi intake induced relatively few cases of myocardial calcification in mdx mice at both 60 and 90 days of age (4 of 30 samples). The form of the crystallization observed in the heart was similar to that of myofiber calcification, although the amount was considerably less (Fig. 6A, C). The incidence of calcification in the heart was absent in mdx fed mid-Pi or low-Pi diets. None of B10 mice fed any of the three types of phosphate diets exhibited myocardial calcification.

As previously described, klotho mutant mice display a number of age-related diseases, including soft tissue calcification. Morishita et al. (2010) reported that klotho mice fed a normal diet show kidney calcification, whereas mice fed a low-Pi diet have reduced precipitation of calcium in the kidneys. We found that a high-Pi intake results in slight ectopic calcification in kidneys of mdx mice (Fig. 6B, D) whereas mdx mice fed mid-Pi or low-Pi diets showed no evidence of calcium deposition in the kidneys. Similar to the findings in the heart, B10 mice under all phosphate diets also showed no calcification in the kidneys.

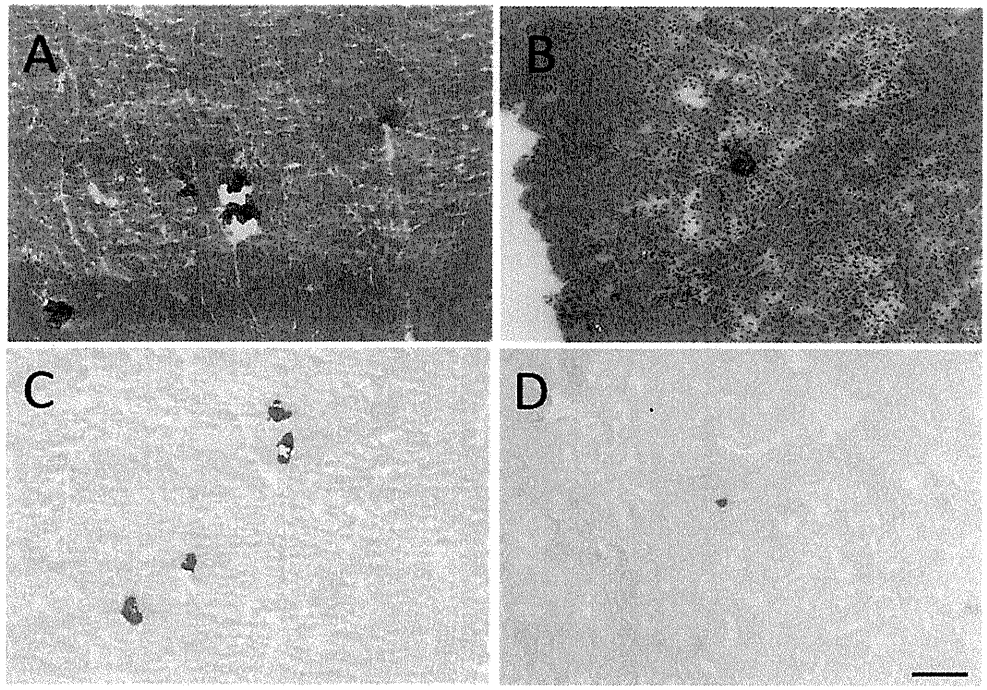

Fig. 6. H&E and alizarin red S-stained cryosections of the heart and kidneys of an mdx mouse fed a high-Pi diet. H&E-stained cryosections of the heart (A) and kidney (B). Alizarin red S-stained cryosections of the heart (C) and kidney (D). The bar represents 10 μm.

5.3 Changes in serum biochemistry

We also examined the serum calcium and phosphate concentrations of B10 and mdx mice fed the three types of Pi diets. The serum phosphate levels of high-Pi fed mdx mice were significantly higher than those of B10 mice fed the same diet, and mdx mice under mid-Pi and low-Pi diets (Fig. 7). However, no marked differences in serum calcium concentrations of mdx mice were detect in the different diet groups. Serum phosphate concentration is largely influenced by dietary intake, with the over-consumption of phosphate often resuting to cause hyperphosphatemia (Calvo et al., 1994), secondary hyperparathyroidism with bone re-sorption (Lutwak et al., 1975), and bone loss (Draper et al., 1979). It is likely that high phosphate intake leads to overworked kidneys and a reduced rate of calcium and phosphate filtration.

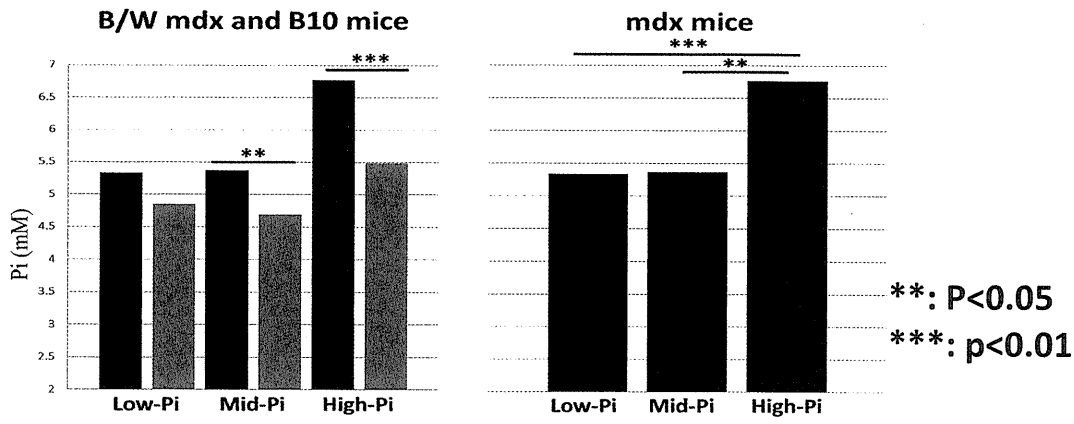

Fig. 7. Serum Pi levels of three-month-old B10 and mdx mice fed three types of Pi diets. Comparison of B10 and mdx mice fed the three Pi diets (left). Comparison among mdx mice (right).

6. Effects of ectopic calcification on muscle function of mdx mice

High-Pi intake induced severe ectopic calcification throughout the skeletal muscle of mdx mice. The presence of ectopic calcification in muscles appeared to have a negative impact on the force output of skeletal muscle. To date, no studies have reported the pathophysiological effects of the accumulation of calcium phosphate in muscles. For this reason, we have investigated the effects of ectopic calcification on skeletal muscle contraction of mdx mice.

For muscle force measurements, *in situ* maximal isometric twitch force and tetanic force of right triceps surae muscle (TSM) were recorded. The isometric force recording system was custom-made and the experimental protocols were based on the design of Dorchies et al. (2006). Sixty-day-old B10 and mdx mice fed the three phosphate diets were lightly anesthetized by diethylether gas and then immobilized on a cork board by covering the bodies with Novix-II (Asahi Techno Glass, Chiba, Japan). A confined area of skin and myofasia of the right hindlimb was cut and exposed, and the sciatic nerve was dissected to induce the analgesic conditions. The knee joint was firmly immobilized by a needle that served as the fulcrum and the Achilles tendon of the leg was then severed and connected to a platinum electrode clip associated with a force transducer (DS2-50N Digital Force Gauge; Imada, Aichi, Japan). A second platinum electrode was directly inserted into the TSM. Experimental trials were started after the animals recovered from anesthesia. Using this procedure, we avoided negative effects (*i.e.* muscle relaxation) of the anesthetic regimen, which we previously confirmed and were able to collect real data without any disturbances. For the measurement of maximal single twitch, muscles were stimulated with a square wave pulse (0.5-msec duration) of stimulation voltage. Tetanic force was measured with 200-msec bursts of frequency set to 100 Hz. Muscle length and weight of TSM were measured to estimate the cross-sectional area (CSA) of the muscle (in mm^2). The specific twitch and tetanic force were normalized by dividing the measured force by the CSA. Using manual settings of the optimal muscle length, maximal twitch contractions were measured within

trials up to 20 contractions and all tetanic force measurements were made at locations where the single twitch force was the greatest.

6.1 Results of maximal single force (MSF) and maximal tetanic force (MTF) measurements

Pre-tests results revealed that B10 mice fed the normal CE-2 diet had significantly stronger maximal single force in response to single-pulse stimulation than that of mdx mice (data not shown). This result is consistent with a previous study by Dorchies et al. (2006). Furthermore, although mdx mice have a heavier body weight and muscle mass of the TSM, they exhibited weaker muscle force compared with the control mice. This finding was also consisted with that reported previously (Quinlan et al., 1992), although the muscle mass of anterior tibial muscle was compared, rather than TSM. Therefore, we are confident that our isometric force recording system can be used to evaluate and compare muscle forces between B10 and mdx mice fed the different phosphate diets (Table 1).

We did not detect any significant differences in twitch force between B10 mice of the three phosphate diets groups. However, the high-Pi diet mdx mice had significantly lower ($P<0.05$) single force than that of mdx mice fed a mid-Pi diet (Fig. 7A), while maximal single force was significantly higher in mdx mice fed a low-Pi diet compared with mid-Pi diet mdx mice. Notably, however, this value was still lower (25% less) than the corresponding value of B10 mice fed a low-Pi diet.

The maximal tetanic force in response to burst stimulation was also measured for all mice. Similar to the results of twitch force, B10 mice had significantly higher tetanic force than mdx mice for all three phosphate diets, whereas no marked differences were detected among B10 mice. Mdx mice fed a high-Pi diet produced significantly less ($P<0.01$) tetanic force than the other mdx mice (Fig. 7B). Based on these findings, we conclude that high-Pi diet has a greater influence on generating the tetanic force in mdx mice than producing twitch force. These results strongly suggest that calcium deposits in muscles interfere with muscle function. The improvement of muscle forces was likely due to the reduction of ectopic calcification because low Pi-diet did not have a positive effect on force generation in B10 mice, which have no ectopic calcification. However, it is also likely that other factors related to dietary phosphate restriction also contribute to improving muscle function.

Mouse	#	Weight (g)	MSF (mN/mm^2)	MTF (mN/mm^2)
Low-Pi B10	7	23.1±1.0	102.5±4.6	344.8±15.2
Low-Pi mdx	7	23.8±1.4	74.2±2.4	254.9±14.6
Mid-Pi B10	7	22.3±0.7	100.0±4.1	341.0±11.1
Mid-Pi mdx	7	25.2±0.5	66.8±1.5	246.4±7.2
High-Pi B10	7	22.8±0.7	101.0±3.3	335.6±6.3
High-Pi mdx	7	23.6±0.7	59.6±2.0	193.9±9.6

Table 1. Results of MSF and MTFmeasurements of B10 and mdx mice for the three Pi diet conditions.

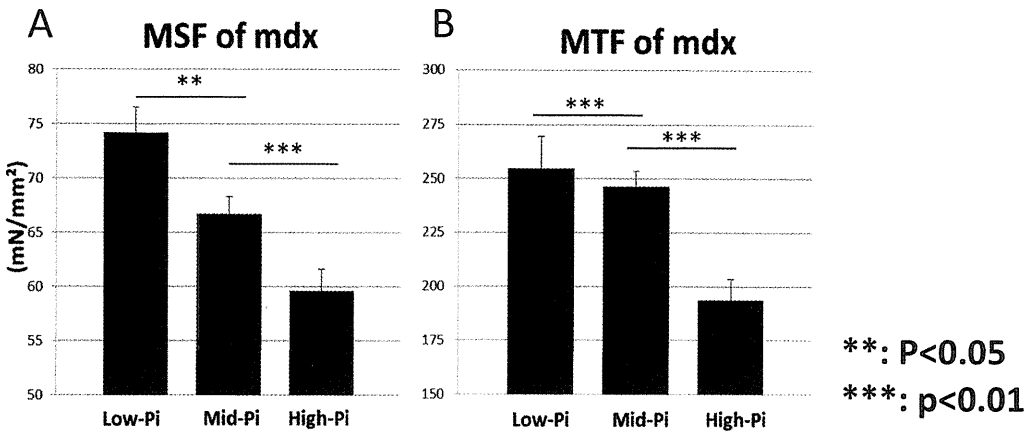

Fig. 8. MSF and MTF measurements of mdx mice for the three Pi diet conditions. (A) Results of MSF. (B) Results of MTF.

7. Reduced calcification by low Pi diet in a longitudinal study

Although the influence of dietary phosphate intake on the precipitation of calcium in mdx mice skeletal muscles has been clarified, the effects of phosphate restriction on severe ectopic calcification remained unclear. To understand the impact of phosphate restriction on the deposition of calcium, a longitudinal study was conducted for four mdx mice raised on high-Pi diet from weaning to 60 days of age. At age of 60 days, whole-body images of the mdx mice were taken by noninvasive CT scanning using a Latheta LTC-200 X-ray micro CT scanner (Aloka Hitachi Medical, Tokyo, Japan) (Fig. 9). The mdx mice were then divided into two groups, a continuously fed high-Pi diet group and a low-Pi diet group, until the age of 90 days, at which point whole-body images of the mice were taken again. The whole-body images and volume density of ectopic calcification in the lower body (from the top of os coxae to ankle joint) were compared (Fig. 10). Mice fed a high-Pi diet displayed an increased volume (0.066 cm^3) of ectopic calcification from 60 to 90 days of age, whereas mdx mice fed a low-Pi diet had a reduced (-0.007 cm^3). Thus, it was concluded that the restriction the restriction of dietary phosphate from the age of 60 days reduced the pre-formed ectopic calcification within one month, while continuously feeding the mice a high-Pi diet led to more severe calcium deposits.

8. Mechanisms of calcification

The complete mechanism underlying progressive muscle degeneration due to dystrophin deficit is unclear. Dystrophin-deficient muscles are highly susceptible to the oxidative stress that results from the early onset of muscle degeneration. Muscle necrosis actively occurs following the degeneration, leading to fibrosis and calcification of muscle fibers (Vercherat et al., 2009). It has been suggested that vascular calcification is actively regulated by osteogenic gene expression in vascular smooth muscle cells (Giachelli, 1999). Attention has been focused on inorganic phosphate as one of the potential factors regulating the observed cellular phenotypic changes, as smooth muscle cells *in vitro* cultured under high-Pi conditions undergo osteogenesis and form calcium deposits (Jono et al., 2000). As skeletal muscle satellite cells possess multilineage potential (Asakura et al., 2001; Wada et al., 2002), they might also undergo osteogenic differentiation under high-Pi conditions.

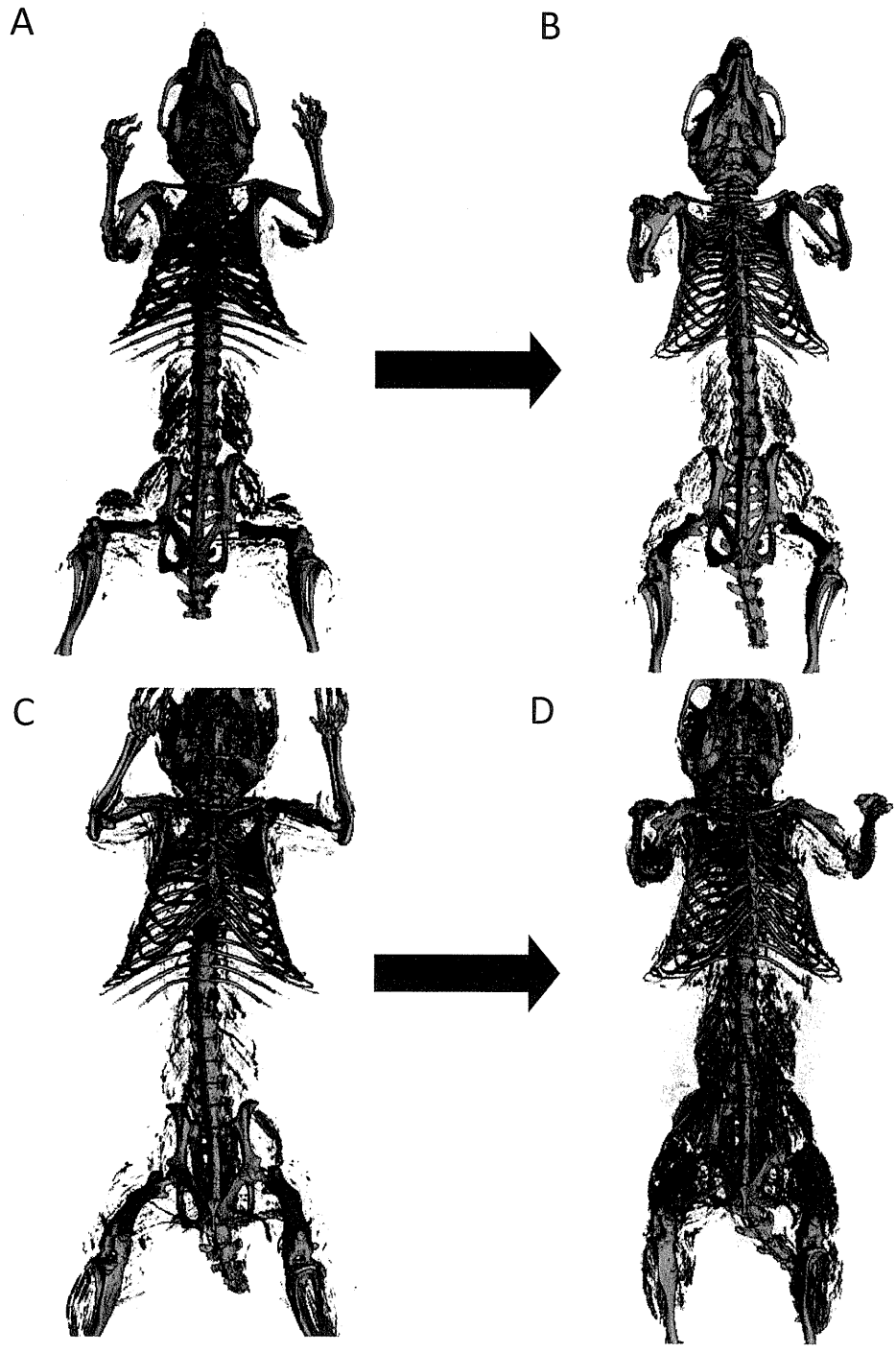

Fig. 9. 3D images of 60-day-old mdx mice fed a high-Pi diet (left) and the images of the same mice after 30 days. (A, B) Sixty-day-old mdx mice fed a high-Pi diet. (C) The same mdx mice (90-day-old) fed a low-Pi diet for 30 days. (D) The same mdx mice (90-day-old) fed a high-Pi diet for 30 days. Bones are shown in grey and ectopic calcification is in light blue.

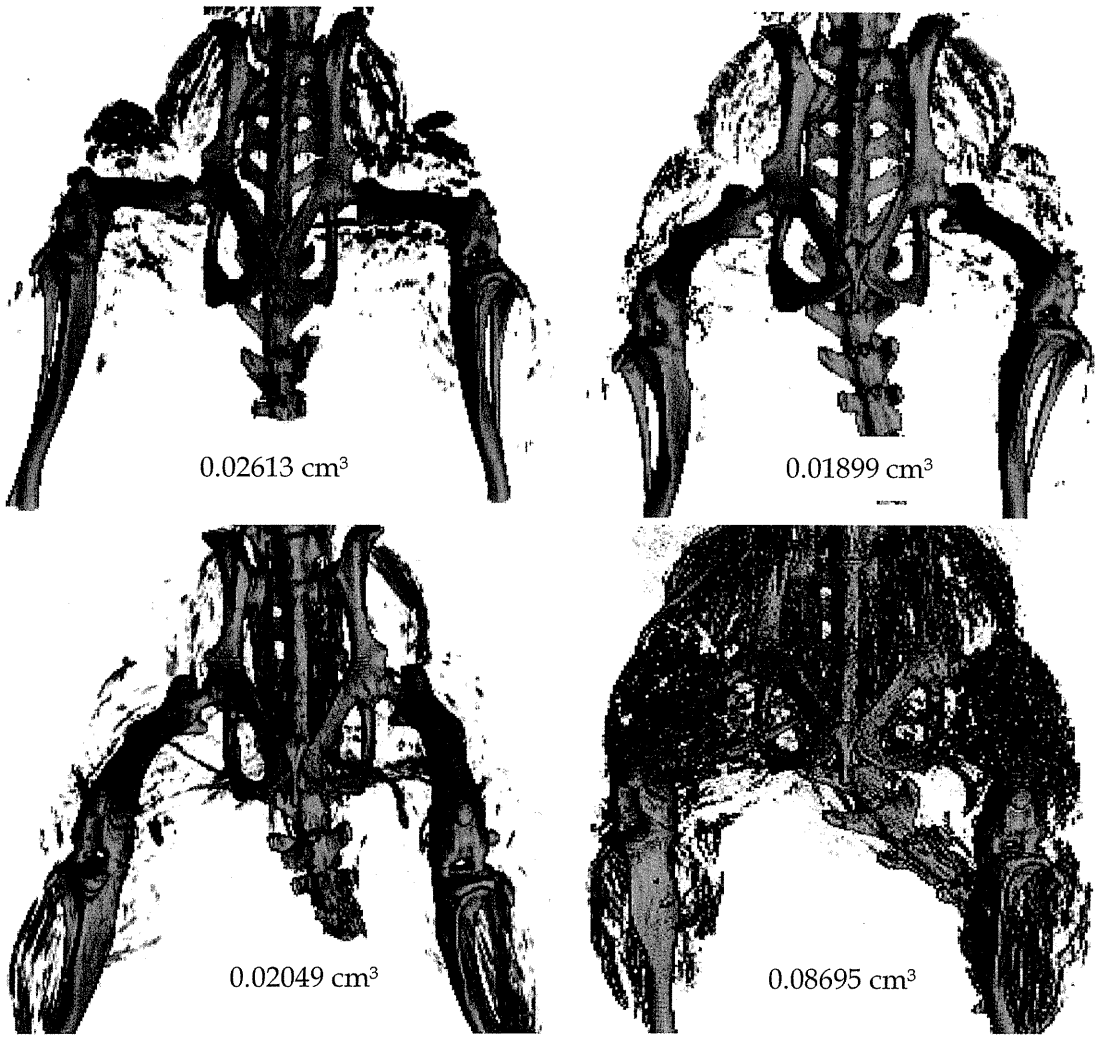

Fig. 10. Enlarged 3D images of the lower limbs of mdx mice fed a high-Pi diet (left) and the images of the same mice fed either low-Pi (top right) or high-Pi diets (bottom right) for 30 days. The numbers represent the volume densities of ectopic calcification in the lower body (from the top of os coxae to ankle joint).

8.1 Pi-induced osteogenesis and reduced myogenesis in C2C12 cells

To study the effects of Pi on muscle cell differentiation, murine myoblast-derived C2C12 cells were cultured for four days under various Pi concentrations and then immunostained for the presence of myogenic (myosin heavy chain; MyHC) and osteogenic (Matrix Gla Protein; MGP) markers. When cultured in normal differentiation medium (Pi=1 mM), the cells underwent muscle differentiation and formed myotubes. Myogenesis proceeded until the Pi concentration of the differentiation medium reached 5 mM, while myotube formation was strongly suppressed at 7 mM. (Fig. 11).

The expression of Runx2, a transcription factor of osteogenesis, increased with the rise of the Pi concentration (Fig. 12A). The retardation of myogenesis caused by the high Pi concentration was also evident by the decrease in both the fusion index and myogenin